Dynamic locational marginal emissions via implicit differentiation

Lucas Fuentes Valenzuela, Anthony Degleris, Marco Pavone, Ram Rajagopal, Abbas El Gamal

***Abstract*—Locational marginal emissions rates (LMEs) estimate the rate of change in emissions due to a small change in demand in a transmission network, and are an important metric for assessing the impact of various energy policies or interventions. In this work, we develop a new method for computing the LMEs of an electricity system via implicit differentiation. The method is model agnostic; it can compute LMEs for almost any convex optimization-based dispatch model, including some of the complex dispatch models employed by system operators in real electricity systems. In particular, this method lets us derive LMEs for *dynamic* dispatch models, i.e., models with temporal constraints such as ramping and storage. Using real data from the U.S. electricity system, we validate the proposed method by comparing emissions predictions with another state-of-the-art method. We show that incorporating dynamic constraints improves prediction by 8.2%. Finally, we use simulations on a realistic 240-bus model of WECC to demonstrate the flexibility of the tool and the importance of incorporating dynamic constraints. Namely, static LMEs and dynamic LMEs exhibit an average RMS deviation of 28.40%, implying dynamic constraints are essential to accurately modeling emissions rates.**

***Index Terms*—Optimal Power Flow, Marginal Emissions, Implicit Differentiation, Optimization**

I. Introduction

Policy-makers interested in decarbonizing the electricity grid require reliable emissions data in order to quantify the impact of a particular policy or intervention strategy. Moreover, the need for this data will only grow as various systems, such as transportation and heating, begin to electrify and place additional strain on the grid. Unfortunately, electricity systems depend on complex, interconnected transmission network structures with numerous operational constraints, making it difficult to attribute emissions to energy consumption at a particular time and place.

Emissions rates are important metrics that quantify the amount of pollutant emissions, e.g., CO_2, SO_2, or NO_x, due to the consumption of energy. Researchers and decision-makers often examine *average emissions rates*, which measure the average rate of emissions per MWh of energy consumed, and *marginal emissions rates* [1], [2] (also known as marginal emissions factors or marginal emissions intensities), which measure the rate at which emissions will increase or decrease given a marginal change in energy demand. While average emission rates quantify emission rates over long periods, marginal emissions rates better quantify the emissions impacts of small, local changes in demand [12], [19], [20] since only a few, specific generators are expected to change production if demand changes slightly. Marginal emissions rates have been used to quantify the impacts of various policies on carbon emissions, e.g., increasing electric vehicle penetration [22], [13], changing electric vehicle charging policies [15], or expanding transmission capacity [21].

Empirical studies on marginal emissions rates in the U.S. and U.K. have used *regression-based approaches* to estimate emissions rates across large geographical regions [12], [20], [10], [4]. These works leverage publicly available data and fit a linear model to changes in emissions and net demand. The main benefit of these

L. Fuentes Valenzuela and A. Degleris are co-first authors. Corresponding author: A. El Gamal.

L. Fuentes Valenzuela, A. Degleris, and A. El Gamal are with the Electrical Engineering Department at Stanford University. R. Rajagopal is with the Civil Engineering Department at Stanford University. M. Pavone is with the Aeronautics and Astronautics Department at Stanford University.

Anthony Degleris is supported by the U.S. Department of Energy, Office of Science, Office of Advanced Scientific Computing Research, Department of Energy Computational Science Graduate Fellowship under Award Number DE-SC0021110.

methods is that they do not require a model of the underlying electricity system. However, because of their inherent data requirements, these methods are difficult to extend to finer geographic resolutions and hypothetical electricity systems that lack preexisting data. Their ability to generalize is yet undetermined.

In contrast, *model-based approaches* explicitly model the electricity system and economic dispatch problem, then derive a formula for nodal marginal emissions rates [5], [18], [17]. The rates, called *locational marginal emissions rates* (LMEs), are the emissions-equivalent of the locational marginal prices, and thereby reveal the impact of network constraints on emissions. Model-based methods are promising because real-world electricity systems are often dispatched using mathematical models, e.g., an optimization problem. Previous work [6] has already used a model-based approach (without network constraints) to predict emissions rates in U.S. grid regions. However, the models used in real world systems are often significantly more complex than those considered in academic research, limiting the applicability of specific derivations in aforementioned studies. In this work, we address this limitation by using a method that supports arbitrary optimization-based dispatch models, including those used in real-world systems.

A. Contribution and outline

This paper makes three main contributions:

- *New method for computing LMEs.* We propose a new method that can compute LMEs in arbitrary convex optimization-based problems. This contrasts with standard regression-based methods, that may have significant data requirements, and previous model-based methods, that cannot account for diverse constraints. The method we propose is generic, flexible, and suitable for real systems dispatched by grid operators.
- *Modeling the effects of dynamic constraints.* We use our method to compute LMEs in networks with dynamic constraints, such as energy storage. We study the impact of these constraints on emissions rates using a realistic model of the Western United States transmission system. The dynamic LMEs are distinct from their static counterparts, demonstrating the importance of accurately including all relevant dynamic constraints when estimating emissions sensitivities.
- *Validation on real data.* We validate the method on a published dataset, and show an improvement in prediction accuracy of changes in emissions provided by the inclusion of dynamic constraints.

The paper is structured as follows. In Section II, we introduce the problem of computing LMEs in dynamic electricity networks. We show that this problem generalizes previous approaches [18], [17] to complex models with temporal constraints. We then show how to solve this problem using implicit differentiation in Section III. Although we use this technique to compute LMEs for the model specified in Section II, our technique generalizes to arbitrary convex optimization-based dispatch models, including those used by system operators in real world electricity markets. Lastly, we report simulation results on two datasets in Section IV. In the first experiment, we demonstrate the validity of our approach on real US electricity data and compare our results with an established method. In particular, by adding unit commitment constraints, we show that our technique can outperform existing methods in predicting changes in emissions. Second, we compute LMEs for a 240-bus model of the Western United States and show that, in the presence of grid-scale storage, dynamic MEFs are essential to accurately quantifying the changes in emissions. We discuss future work in Section V.

II. Problem formulation

In this section, we formulate the problem of computing the LMEs in a dynamically constrained electricity system. First, Section II-A provides background information on the *dynamic dispatch problem*, a mathematical model for electricity networks with temporal constraints. We then describe our mathematical model for emissions and marginal emissions in static networks in Section II-B, where we formally state the dynamic marginal emissions problem. Finally, in Section II-C, we describe two special cases of the dynamic marginal emissions problem that have been solved in previous work. Notably, both special cases are static, i.e., they do not incorporate any dynamic constraints.

A. Dynamic dispatch model

In electricity systems, a *dispatch model* is a mathematical model for deciding which electricity generators should be used to meet demand. Dispatch models are often formulated as convex optimization problems, where the variables are the amount of power produced by each generator, and the parameters include both the current electricity demand and the physical constraints of the system. When modeling emissions, researchers often consider *static* dispatch models, models that only reflect a single instant in time. However, most real world electricity systems have *dynamic* constraints—constraints that couple generator outputs across time periods. For example, a generator with ramping constraints can only change its power output by a small amount between successive time periods. In order to effectively model the impact of temporal constraints on emissions, we will study the *dynamic optimal power flow problem*,

$$\begin{array}{ll} \text{minimize} & \sum_{j=1}^{k} f_j(g_j) \\ \text{subject to} & g_j \in \mathcal{G}_j, \quad j \in [1:k], \\ & D\mathbf{1} = G\mathbf{1} \\ & (D - BG)F \leq F^{\max} \end{array} \tag{1}$$

where the variable is $G \in \mathbf{R}^{T \times k}$ with columns $g_1, \ldots, g_k$. The matrix G represents the power output of k devices over T timesteps; each device can supply power, store power, or otherwise interact with the grid. The entry G_{tj} represent the output of device $j \in [1:k]$ at time t.

a) Device Costs and Constraints.: Each device j has three properties: a convex cost function $f_j(g) : \mathbf{R}^T \to \mathbf{R}$, a convex constraint set $\mathcal{G}_j \subset \mathbf{R}^T$, and a location on the network. We model the device locations with a matrix $B \in \{0,1\}^{n \times k}$ that maps each device to a particular node in the network, i.e., $B_{ij} = 1$ if device j is located at node i, and $B_{ij} = 0$ otherwise. The objective of Problem (1) is to minimize the sum of the device costs, and the first constraint states that each device must stay within their constraint set.

b) Network Constraints.: Problem (1) considers an electricity network with n nodes and m edges (transmission lines). Node $i \in [1:n]$ has demand D_{ti} at time $t \in [1:T]$. The second constraint is that power must be balanced across the network, i.e., $D\mathbf{1} = G\mathbf{1}$. Finally, the third constraint is that the power flowing across each transmission line is limited by its capacity. We define $F \in \mathbf{R}^{n \times m}$ to be the *power flow distribution factor matrix*, where $F_{i\ell}$ determines how a power injection at node i (withdrawn at node n) affects power flow across line $\ell \in [1:m]$. Because of thermal and voltage phase angle constraints, each line ℓ can only transport up to $F_{\ell t}^{\max}$ units of power at time t, modeled with the constraint $(D - BG)F \leq F^{\max}$.

c) Solution Map.: We denote $g_i^*(D) : \mathbf{R}^{Tn} \to \mathbf{R}^T$ the optimal schedule for generator i as a function of demand (here, we abuse notation and treat D as a vector in $\mathbf{R}^{Tn}$ when it is the argument of a function). We assume that $g_i^*(D)$ exists and is unique for all $D \in \mathbf{R}^{Tn}$. In other words, we assume problem (1) has a unique solution for all $D \in \mathbf{R}^{Tn}$. This assumption is made without loss of generality. We call g_i^* the *solution map*. As we will see shortly, the solution map will allow us to formalize the relationship between demand and emissions.

B. Locational marginal emissions

We model the emissions of generator i as a linear function of power output with rate c_i Although we use a linear model throughout the remainder of the paper, it is straightforward to generalize all our results to nonlinear models. Since the generator power outputs are determined by the dispatch model, the emissions at time t generated as a function of demand is $E_t(D) = \sum_i c_i(g_i^*(D))_t$. The *total emissions* is then $E(D) = \sum_{t=1}^{T} E_t(D)$.

a) Problem statement.: The LMEs $\Lambda(D) : \mathbf{R}^{Tn} \to \mathbf{R}^{Tn}$ are the marginal rate of change in total emissions given a marginal change in demand. In other words, the LMEs are the gradient of emissions with respect to demand, i.e., $\Lambda(D) = \nabla E(D)$; since the marginal emissions rates are the local rate of change of $E(D)$, the derivative $\Lambda(D) = \nabla E(D)$ defines the locational marginal emissions rates.

The function $\Lambda(D)$ is vector-valued, since changes in electricity consumption at different nodes and different times may have different impacts on emissions. The problem we study in this paper is how to compute $\Lambda(D)$ when the solution maps $g_i^*(D)$ are determined by the dynamic optimal power flow problem.

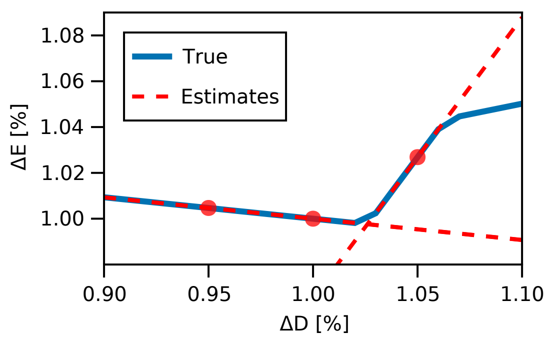

Fig. 1. Illustration of marginal emission rates. (Solid blue curve) Total emissions as a function of demand at a particular node. (Dashed red curves) Predicted total emissions using the LMEs computed at each red circle. The LMEs are the slopes of the dashed red curves.

C. Special Case: Static Generators

When we restrict the devices (the functions f_i and sets $\mathcal{G}_i$) to be static generators, we recover previous analytical models [5], [18], [17]. The static generator device has constraint set $\mathcal{G} = \{g \mid g^{\min} \leq g \leq g^{\max}\}$, where $g^{\min}, g^{\max} \in \mathbf{R}^T$ and cost function $f(g) = \sum_t a g_t^2 + b g_t$. The static generator could represent a traditional dispatchable generator, in which case $g^{\max} = c\mathbf{1}$, or a renewable resource, in which case the entries of $g^{\max}$ may vary. Most importantly, the static generator has no temporal constraints: g_t is independent of the choice of $g_{t'}$ when $t \neq t'$. In a network with only static generator devices, the dynamic problem would simplify to T *static* optimal power flow problems that can be solved independently.

If all the devices in Problem (1) are static generators, then Problem (1) reduces to the model considered in [18]. Moreover, if we remove the network constraints by setting $F = 0$, we recover the model used in [6] to empirically estimate emissions rates.

D. Dynamic Devices

By addressing the dynamic optimal power flow problem in its full generality, our framework allows us to consider dynamic devices as well. These devices have temporal constraints, implying their actions at any given time depend on their actions at other times. We give three examples below.

a) Ramp-constrained generators: Ramping constraints limit the rate at which a generator can change its output. These generators are modeled with the constraint set,

$$\begin{aligned} \mathcal{G} = \{ \ g \ | g^{\min} \leq g \leq g^{\max}, \\ g_t - \rho \leq g_{t+1} \leq g_t + \rho, t \in [1:T-1] \ \} \end{aligned}$$

where $\rho \in \mathbf{R}^k$ is the ramping rate of each generator. Ramp-constrained generator devices have the same cost functions as static generator devices, $f(g) = \sum_t a g_t^2 + b g_t$. Ramping constraints are particularly useful in dynamic dispatch models with short time intervals, e.g., 15 minutes, and slow dispatching generators, like nuclear and hydro.

b) Storage devices: Storage devices include pump-hydro resources, grid-scale batteries, and DER aggregators selling storage services to the grid. We define a storage device to have cost function $f(g) = 0$ and constraint set $\mathcal{G}$ that is the set of $g \in \mathbf{R}^T$ such that there exists $s, \gamma, \delta \in \mathbf{R}^T$ satisfying for $t \in [1:T]$

$$\begin{aligned} 0 \leq s \leq C, \qquad 0 \leq \gamma \leq P, \qquad 0 \leq \delta \leq P, \\ g_t = \delta_t - \gamma_t, \qquad s_t = s_{t-1} + \eta\gamma_t - (1/\eta)\delta_t \end{aligned}$$

where $s_0 = 0$. The vector $C \in \mathbf{R}$ is the storage capacity, $P \in \mathbf{R}$ is the maximum (dis)charge rate, and $\eta \in (0, 1]$ is the storage efficiency.

c) Unit commitment-constrained generators: Unit commitment constraints are integer constraints specifying whether or not a power generator is on. If generator i is on, it must produce a minimum power $g_i^{\min}$ and stay on for a specified period of time. We model this by modifying the generator device constraint set to be the set $\mathcal{G} = \mathcal{G}_{\text{static}} \cup \{0\}$, where $\mathcal{G}_{\text{static}}$ is the equivalent static generator. Although the set $\mathcal{G}$ is not convex, it can be made convex by introducing an integer variable $z \in \{0, 1\}$. The integer constraint makes (1) a mixed-integer convex program, and hence NP-hard. Fortunately, many good heuristics for solving mixed-integer convex programs are readily available through commercial solvers such as Gurobi [11].

III. Implicit Differentiation-Based Marginal Emission Rates

In previous model-based studies, marginal emissions rates are derived by first calculating how generation changes with demand, and then multiplying the change in generation by the emissions rate of each generator. This is a manifestation of the chain rule, which states that $\Lambda(D) = \nabla E(D) = \sum_{t=1}^{T} Jg_t^*(D)^T c$. Therefore, the main technical challenge when computing $\Lambda(D)$ is computing an analytical expression for the Jacobians $Jg_t^*(D)$. In previous studies that only consider static dispatch models, i.e., $T = 1$, one only needs to derive an expression for $Jg_1^*(D) \in \mathbf{R}^{k \times n}$.

In the general setting, the situation is much more complex—one must derive T Jacobians of size $k \times Tn$. Although deriving an analytical expression is certainly possible, we take a simpler and more powerful approach in this paper: we use the *implicit function theorem* to compute the Jacobians $Jg_t^*(D)$.

Theorem 1 (Implicit Function Theorem)**.** *Suppose* $K : \mathbf{R}^n \times \mathbf{R}^r \to \mathbf{R}^k$ *is strictly differentiable at* $(D_0, x_0) \in \mathbf{R}^n \times \mathbf{R}^r$ *and* $K(D_0, x_0) = 0$*. Moreover, suppose the partial Jacobian* $J_x K(D_0, x_0)$ *is nonsingular. Then the solution mapping* $x^*(D) = \{x \in \mathbf{R}^r \mid K(D, x) = 0\}$ *is single-valued in a neighborhood around* (D_0, x_0) *and strictly differentiable at* (D_0, x_0) *with Jacobian*

$$Jx^*(D_0) = -J_x K(D_0, x_0)^{-1} J_D K(D_0, x_0).$$

The implicit function theorem states that if a differentiable system of equations $K(D, x) = 0$ has a solution at (D_0, x_0), and the corresponding partial Jacobian $J_x K(D_0, x_0)$ is non-singular, then the solution map $x^*(D)$ is a locally well-defined function with Jacobian given by Theorem 1. In our setting, the solution map $G^*(D)$ is not the solution to a system of equations, but rather the solution to a convex optimization problem. In this case, a *fixed point mapping* defines the solution to the problem, via the Karush-Kuhn-Tucker (KKT) conditions.

By constructing the optimization problem so that the KKT conditions are strictly differentiable and that the solution $G^*(D)$ always exists and is unique, we can guarantee the conditions of Theorem 1 are satisfied, and derive a general expression for the Jacobian of the solution map. Combining this with the chain rule, we can then derive marginal emissions rates for the dynamic optimal power flow problem.

a) Remark: Since the dynamic OPF problem includes the static OPF problem and the economic dispatch problem as special cases, this work generalizes the derivations in [18] and [6]. However, our method is by no means constrained to the dynamic dispatch model used in this paper; implicit differentiation can be used to derive the marginal emissions rates for nearly any convex-optimization based dispatch model. Importantly, this includes many of the dispatch models used by system operators in practice, a point we revisit in Section V.

A. Complexity and Software Implementation

We implement our method in Julia [3] for all the aforementioned dispatch models and constraints. Our implementation is publicly available on Github. We use `Convex.jl` [23] to model the problem and solve it with external solvers, such as ECOS [7] or Gurobi [11]. For the large-scale network discussed in Sections IV-B and IV-C (i.e. $n = 240$ nodes, $k = 136$ generators, $m = 448$ lines) and $T = 1$ time periods, our software package solves the dispatch problem and computes the resulting LMEs in just under a second on a modern laptop with a 2.3 GHz quad-core processor. For the same problem with $T = 24$ time periods, the same machine takes about two minutes to solve the problem and compute the LMEs.

Our software package offers a flexible interface and can be used to analyze networks with different physical characteristics (e.g, location of generators, transmission line ratings) and constraints (e.g., ramping rates). After specifying the network parameters, computing LMEs can be obtained with a single function call. Because our implementation is open-source, reasonably fast, and easy to use, we believe it is of value to the broader community.

In general, we expect our method to scale well to realistic problems encountered by grid operators. Specifically, solving the dispatch problem requires $O(z^4)$ operations, constructing the Jacobian requires $O(z^2)$ operations, and inverting the Jacobian to compute the emissions rates requires $O(z^3)$ operations, where $z = T \cdot \max(m, n, k)$. Since many grid operators already solve large dispatch problems at regular intervals (e.g., every 15 minutes to clear the real-time market) and solving the dispatch problem is the most computationally intensive step, our method should scale well to large, real networks

IV. Simulation Results

In this section, we illustrate the applicability and utility of the suggested approach in two different settings. First, in Section IV-A, we use dynamic constraints to improve MEF prediction in aggregated real data from the U.S. Western Interconnection. Specifically, we reproduce the model from [6] and add unit commitment constraints to coal-powered generators in order to improve emissions prediction accuracy. Second, we illustrate the methodology on a recent reduced network model of the same region [24]. Using the original dataset, we highlight the geographic variance of marginal emissions across the network. Then, we investigate the potential impacts of hypothetically large renewable penetration of storage and renewable generation.

A. Economic Dispatch in the Western United States

In our first experiment, we analyze electricity data from the U.S. Western Interconnection system in 2016. The Western Interconnection dataset is compiled in [6] and contains weekly generator capacities, generator costs, and generator emission rates for large (above 25 MW capacity) fossil fuel generators in the Western Interconnection, as well as hourly total demand and total carbon emissions. Because no transmission data is available, we consider models without transmission constraints. We compare our model to results from [6] and show that the addition of unit-commitment constraints improves emissions prediction accuracy.

a) Models: We analyze two models, which we compare to a baseline. First, we analyze the results of the simple economic dispatch model (1), with linear costs $f_i(g_i) = b_i g_i$, where b_i is the marginal operation cost of generator i. Second, we analyze a dynamic economic dispatch model with unit commitment constraints, over a time horizon of $T = 24$. The unit commitment constraints are only applied to coal generators, all of which are given a minimum output of $g_i^{\min} = 0.4 g_i^{\max}$. The *reduced-order dispatch model (RODM)* described in [6] is used as a baseline. The core of the RODM is a *merit order*-based dispatch process: generators are dispatched in ascending order of cost. After dispatching generators via the merit-order, the *marginal generator*—the generator next in line to modify its output to meet an increase in demand—is identified to find the marginal emissions rate of the system. In [6], post-processing steps are applied to generate the marginal emission rates. Notably, when no post-processing is applied, the RODM is identical to the economic dispatch model in (1) with linear costs $f_i(g_i) = b_i g_i$.

b) Results: After generating LMEs λ_t for every hour $t = 1, \ldots, T$ of the year, where $T = 8760$, we use the resulting marginal emissions rates to predict hourly changes in emissions. Specifically, we compute the historical change in demand Δd_t and change in emissions ΔE_t for every hour of the year. Each model's predicted change in emissions if given by $\Delta \hat{E}_t = \lambda_t \Delta d_t$. In order to compare the predictions of different models, we compute the absolute error $|\Delta \hat{E}_t - \Delta E_t|/Z$ of each model's prediction at each timepoint, where errors are normalized by the mean absolute change in emissions $Z = \frac{1}{T}\sum_{t=1}^{T} |\Delta E_t|$. We use absolute error, instead of square error, to minimize the effect of outliers.

A violin plot of absolute errors is displayed in Figure 2, Panel A. As expected, the economic dispatch model and the model from [6] perform similarly—the model from [6] only differs from the economic dispatch model in its post-processing. Notably, the unit commitment model outperforms both economic dispatch and [6] in predicting changes in emissions (an approximately 7% reduction in normalized mean absolute error). We attribute this to the fact that the unit commitment model accurately models constraints that appear in real world dispatch processes, namely that coal generators cannot rapidly turn on and off again.

LMEs as a function of demand are also reported in Panel B of Figure 2. Historical LMEs are computed as $\lambda_t = \Delta E_t / (\Delta d_t + \epsilon)$, where $\epsilon = 0.5$ MWh is a small value used to avoid unreasonably large LMEs when Δd_t is small. Following a similar procedure to [6], the LMEs for the data and for each model are smoothed using the mean of a rolling window of 20% of the data. Shaded regions representing the interquartile range (IQR) of the data are also plotted to better understand the variance of each model. After averaging, the LMEs produced by the economic dispatch model most closely resemble the data. However, the variation is significantly reduced in the unit commitment model, and the IQR most closely resembles that of the data compared to both other models.

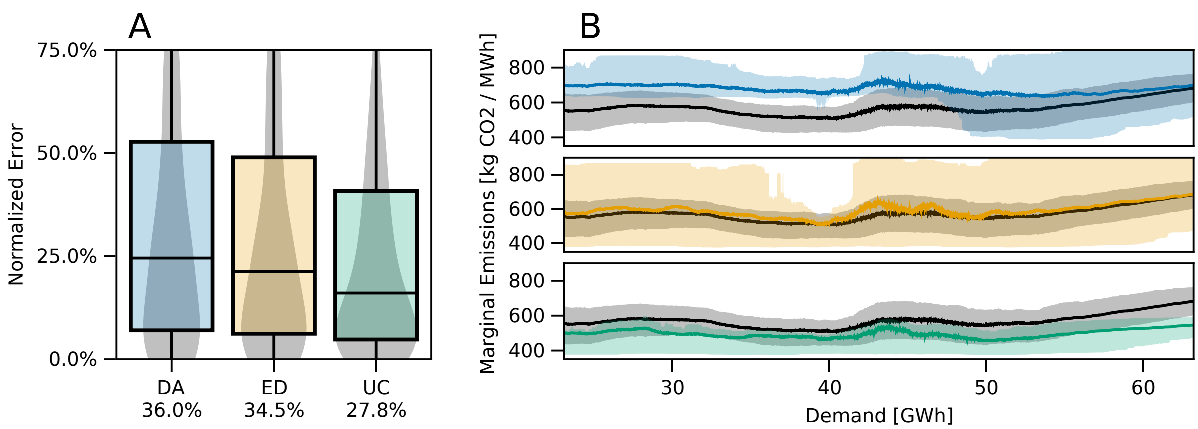

Fig. 2. (Panel A) Emissions prediction error for model from [6] (DA), economic dispatch model (ED), and unit commitment model (UC), normalized by the mean absolute change in emissions. The ED model, effectively the same as the DA model without post-processing, performs similarly. The UC model significantly reduces the prediction error compared to [6], suggesting unit commitment more accurately represents the real world dispatch process. (Panel B) LMEs as a function of total demand. Emissions rates are smoothed using the mean of a rolling window of 20% of the data. Shaded regions represent the interquartile range (IQR) of the rolling window (middle 50% of the data).

B. 240-bus Network Model

In this experiment, we study LMEs using a recent 240-bus network that models the Western United States in 2018 [24]. The dataset includes generator capacities, costs, and ramping rates; hourly demand and renewable generation for $T = 8760$ hours; and the efficiencies and capacities of four pumped hydro storage units. We solve the dispatch problem and compute hourly LMEs using a dynamic model with storage devices as described in Section II. We use this experiment to demonstrate the impact of network constraints on the LMEs. Since the network has relatively little storage and only a few generators have ramping constraints, we do not analyze the impact of storage and dynamic constraints in this experiment.

The distribution of LMEs at 6pm in July is reported in Figure 3, Panel A. In the case of low renewable and storage penetration, we observe that, on average, LMEs are narrowly centered around the mode of the distribution. A geographic distribution of LMEs throughout the network for the month of July at 6pm is reported in Figure 3, Panel B. As is the case for LMPs, we observe a high locational dependence of marginal emissions rates. This clearly illustrates how transmission constraints can often cause local geographic discrepancies in LMEs. For example, despite their geographic proximity, the California Bay Area differs significantly from the Sacramento area. Local diversity in LMEs emphasizes the importance of modeling the network when computing emissions rates: a small geographic change can cause large differences in emissions rates. Demand-centered measures for emissions reductions need to take this variability into account.

C. High Renewable Scenario in the 240-bus Network

To illustrate the impact of grid-level changes on emissions, a high-renewable version of the 240-bus network is presented in this section. Specifically, we uniformly scale renewable generation in the original 2018 model so that renewable generators meet 27% of total demand (compared to 13.5% originally). We also add 15 GW of 4-hour battery storage distributed among the ten largest renewable nodes proportional to generation capacity. These batteries have a round trip efficiency of 89.8% with symmetric charging and discharging efficiencies and are constrained to start and end each day with 50% of their total capacity. As in Section II, we assume the grid operator manages these batteries to minimize the

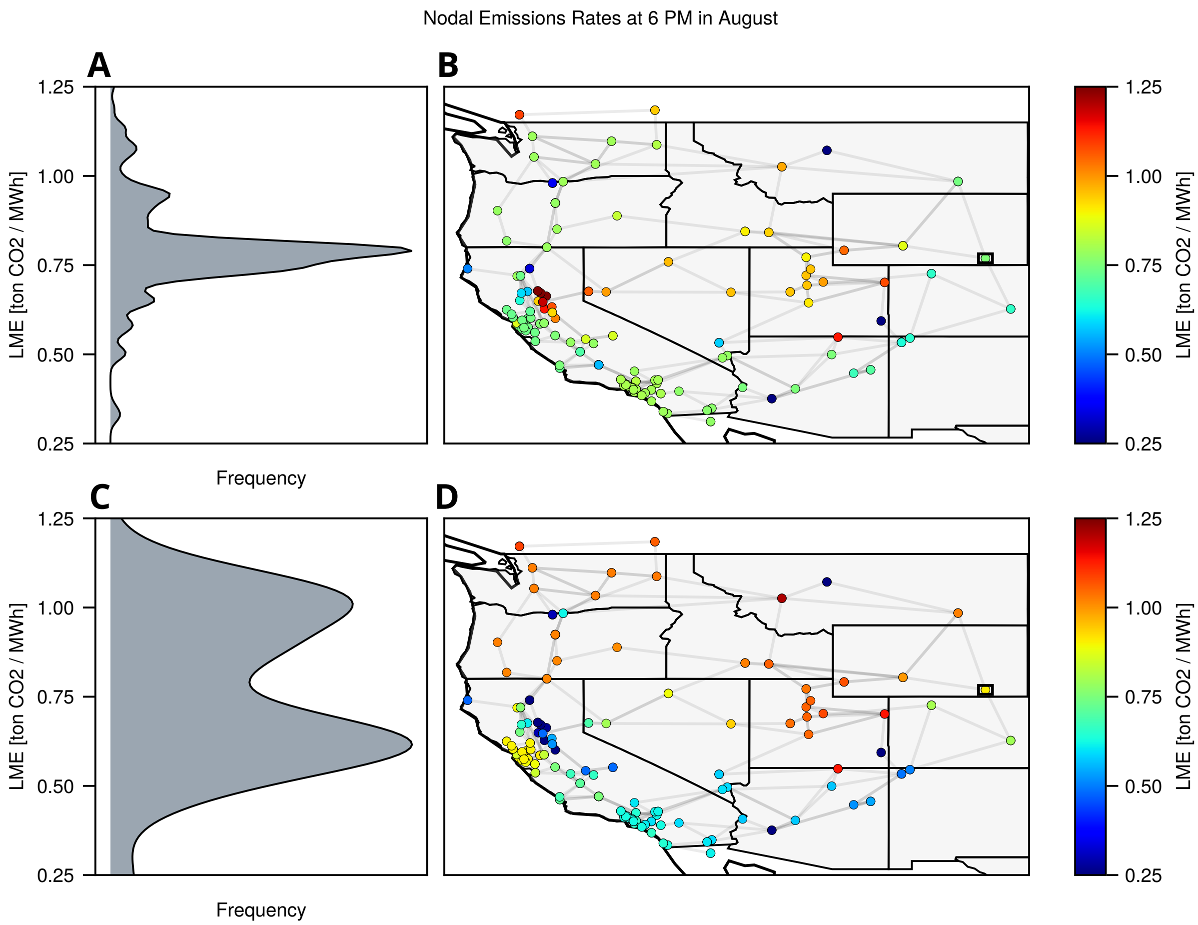

Fig. 3. (Panel A) Distribution of LMEs at 6 PM in August 2018 in the 240-bus WECC network. We display the distribution of LMEs across all nodes. (Panel B) A map of (average) nodal LMEs through the 240-bus WECC network. (Panels C and D) Same as Panels A and B, but for the high renewable scenario with 15 GW of 4-hour storage.

overall cost of electricity. Panels C and D in Figure 3 report the distribution of LMEs as well as their locational dependencies for the month of July in the high renewable scenario. Significant differences appear throughout the network; in general, the LMEs are lower and vary more widely across the network.

In order to highlight the value of explicitly integrating dynamic constraints, we compare the true dynamic LMEs to the analagous 'static LMEs' that arise from eliminating dynamic constraints. Specifically, after solving the dynamic dispatch problem, we fix the battery charging and discharging schedules, and hence eliminate the dynamic constraints. We then compute the LMEs of the resulting model, which now only has static devices and constraints. The difference between true, dynamic LMEs and static LMEs represents the importance of modeling dynamic devices when computing marginal emissions rates. We report these differences in Figure 4, Panel A, where we display the distribution across all nodes and all days of the year of the root mean squared (RMS) deviation between the vector of daily emissions

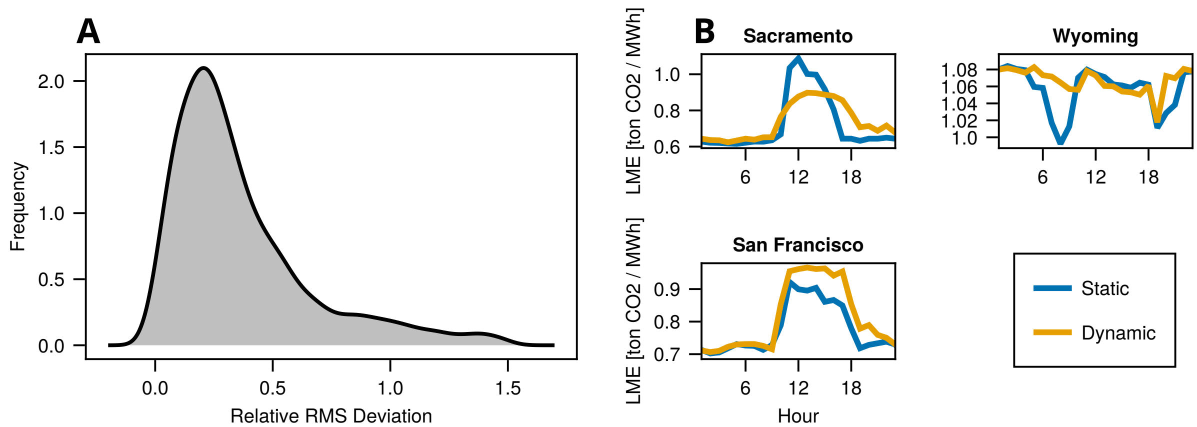

Fig. 4. (Panel A) Distribution of root mean squared deviation between nodal LMEs produced by the static model and the dynamic model, normalized relative to the scale of the LMEs. The average RMS deviation between the static and dynamic model is 28.40%. (Panel B) Hourly time series of static LMEs (blue) and dynamic LMEs (yellow) during three sample days.

rates for the static model, $\lambda_{\text{static}} \in \mathbf{R}^{24}$, and they dynamic model $\lambda_{\text{dynamic}} \in \mathbf{R}^{24}$. The distribution of RMS deviations, with an median RMS deviation of 28.40%. Both metrics are therefore very different, indicating for a need to account for dynamic effects across timesteps. In Panel B, we illustrate the static and dynamic LMEs for four randomly sampled days. While static LMEs are very good approximation in some instances (e.g., top right), they deviate significantly in others. These two results suggest that ignoring dynamic constraints and simply computing static LMEs is not an accurate approximation of dynamic networks: explicitly computing dynamic LMEs are essential to understanding emissions rates in systems with significant storage capacity.

V. Conclusion

In this paper, we introduce a novel method for computing locational marginal emissions rates using implicit differentiation. We use this method to compute the LMEs of dynamic dispatch models, i.e., dispatch problems containing temporal constraints. Incorporating dynamic constraints is shown to improve prediction of historical changes in emissions compared to previous studies. We also observe that LMEs in models with temporal constraints are sometimes hard to approximate by their static counterparts, particularly in networks with high renewable and storage penetration. Since flexible loads and energy storage are expected to play a large role in future grids, we believe incorporating dynamic constraints will be essential to accurately modeling LMEs.

The method presented in this paper generalizes previous methods to arbitrary convex optimization-based dispatch models. Since many system operators use convex optimization-based dispatch models in day ahead and real time electricity markets [16], they could use this method to publish marginal emissions factors in real time. Although these models can be notably more complex than those analyzed in academic research, the proposed method can compute marginal emissions factors for any such model, as long as they can be cast as convex optimization programs. Moreover, by leveraging automatic differentiation software and optimization modeling languages [9], the system operator would only need to specify the objective and constraints of their dispatch problem. LMEs could then be published alongside LMPs to provide real time emissions information to electricity market participants. This could be helpful, for example, to a large internet company choosing to reduce emissions by directing internet traffic to servers in low emitting regions, a problem considered in [14].

Finally, we comment on two directions for future work. First, our paper shows how to compute LMEs when the full network model is available. In some cases, however, the network model may be unavailable to the interested party. Understanding how to estimate the parameters of the electricity network from publicly available data (using the methods developed in [8], for example) and then deriving marginal emissions factors from the learned model is an interesting area of research. Second, we note that computing LMEs in large networks could be computational intensive. Exploiting network structure and using distributed computation could yield significant performance gains.

ACKNOWLEDGEMENTS

The authors thank Liang Min and Inês Azevedo for their valuable comments and suggestions.

REFERENCES

[1] Marginal Emissions Methodology – Watttime.

[2] WattTime Validation and Technology Primer.

[3] Jeff Bezanson, Alan Edelman, Stefan Karpinski, and Viral B Shah. Julia: A Fresh Approach to Numerical Computing. *SIAM Review*, 59(1):65–98, 1 2017.

[4] Duncan Callaway, Meredith Fowlie, and Gavin Mccormick. Location, Location, Location: The Variable Value of Renewable Energy and Demand-side Efficiency Resources. 2017.

[5] Antonio J. Conejo, Enrique Castillo, Roberto Mínguez, and Federico Milano. Locational marginal price sensitivities. *IEEE Transactions on Power Systems*, 20(4):2026–2033, 2005.

[6] Thomas A. Deetjen and Inês L. Azevedo. Reduced-Order Dispatch Model for Simulating Marginal Emissions Factors for the United States Power Sector. *Environmental Science and Technology*, 53(17):10506–10513, 2019.

[7] Alexander Domahidi, Eric Chu, and Stephen Boyd. ECOS: An SOCP solver for embedded systems. In *2013 European Control Conference (ECC)*, pages 3071–3076. ieeexplore.ieee.org, 7 2013.

[8] Priya L Donti, Inês Lima Azevedo, and J Zico Kolter. Inverse Optimal Power Flow: Assessing the Vulnerability of Power Grid Data. *phys2018.csail.mit.edu*, 2018.

[9] Iain Dunning, Joey Huchette, and Miles Lubin. JuMP: A Modeling Language for Mathematical Optimization. *SIAM Review*, 59(2):295–320, 1 2017.

[10] Joshua S. Graff Zivin, Matthew J. Kotchen, and Erin T. Mansur. Spatial and temporal heterogeneity of marginal emissions: Implications for electric cars and other electricity-shifting policies. *Journal of Economic Behavior & Organization*, 107(PA):248–268, 11 2014.

[11] L L C Gurobi Optimization. Gurobi Optimizer Reference Manual, 2022.

[12] A. D. Hawkes. Estimating marginal CO2 emissions rates for national electricity systems. *Energy Policy*, 38(10):5977–5987, 2010.

[13] Patrick Jochem, Sonja Babrowski, and Wolf Fichtner. Assessing CO2 emissions of electric vehicles in Germany in 2030. *Transportation Research Part A: Policy and Practice*, 78(2015):68–83, 2015.

[14] Julia Lindberg, Yasmine Abdennadher, Jiaqi Chen, Bernard C Lesieutre, and Line Roald. A Guide to Reducing Carbon Emissions through Data Center Geographical Load Shifting. In *Proceedings of the Twelfth ACM International Conference on Future Energy Systems*, e-Energy '21, pages 430–436, New York, NY, USA, 6 2021. Association for Computing Machinery.

[15] Ivan Pavić, Tomislav Capuder, Ninoslav Holjevac, and Igor Kuzle. Role and impact of coordinated EV charging on flexibility in low carbon power systems. *2014 IEEE International Electric Vehicle Conference, IEVC 2014*, 2015.

[16] PJM. PJM Manual 12: Balancing Operations. 2021.

[17] Aleksandr Rudkevich and Pablo A. Ruiz. Locational Carbon Footprint of the Power Industry: Implications for Operations, Planning and Policy Making. pages 131–165, 2012.

[18] Pablo A. Ruiz and Aleksandr Rudkevich. Analysis of marginal carbon intensities in constrained power networks. *Proceedings of the Annual Hawaii International Conference on System Sciences*, pages 1–9, 2010.

[19] Wouter Schram, Ioannis Lampropoulos, Tarek Alskaif, and Wilfried Van Sark. On the Use of Average versus Marginal Emission Factors.

[20] Kyle Siler-Evans, Inês Lima Azevedo, and M. Granger Morgan. Marginal emissions factors for the U.S. electricity system. *Environmental Science and Technology*, 46(9):4742–4748, 2012.

[21] Yanlong Sun, Chongqing Kang, Qing Xia, Qixin Chen, Ning Zhang, and Yaohua Cheng. Analysis of transmission expansion planning considering consumption-based carbon emission accounting. *Applied Energy*, 193:232–242, 2017.

[22] Fan Tong and Inês M.L. Azevedo. What are the best combinations of fuel-vehicle technologies to mitigate climate change and air pollution effects across the United States? *Environmental Research Letters*, 15(7), 2020.

[23] Madeleine Udell, Karanveer Mohan, David Zeng, Jenny Hong, Steven Diamond, and Stephen Boyd. Convex Optimization in Julia. In *2014 First Workshop for High Performance Technical Computing in Dynamic Languages*, pages 18–28. ieeexplore.ieee.org, 11 2014.

[24] Haoyu Yuan, Reetam Sen Biswas, Jin Tan, and Yingchen Zhang. Developing a Reduced 240-Bus WECC Dynamic Model for Frequency Response Study of High Renewable Integration. In *2020 IEEE/PES Transmission and Distribution Conference and Exposition (T D)*, pages 1–5. ieeexplore.ieee.org, 10 2020.